Available online at www.sciencedirect.com
ScienceDirect
Computers and Mathematics with Applications 55 (2008) 230–234
An International Journal
computers & mathematics
with applications
www.elsevier.com/locate/camwa

The effect of sidewall friction on dense granular flows

Nicolas Taberlet*, Patrick Richard, Renaud Delannay

Groupe Matière Condensée et Matériaux, UMR CNRS 6626, F-35042 Rennes cedex, France

Received 8 November 2006; accepted 5 April 2007

Abstract

We present novel results on flow properties using molecular dynamics simulation as well as γ-densitometry experiments. We show that fundamentally different types of granular flow can be observed in one unique system. Using both frictional and frictionless confining walls, we show that the differences existing between these regimes originate in the frictional properties of the walls. The salient features of each regime are described in detail. In particular, the packing fraction and streamwise velocity profiles are shown to hinge on the frictional properties of the confining walls. Finally, we propose a dimensionless number, independent of the grain size, which helps to delineate the different regimes.

1. Introduction: Granular flows on an erodible pile

Due to the fundamental interest as well as the numerous industrial applications [1], a great deal of both experimental [2–4] and theoretical [5] work has been devoted to the rheology of dry granular flows confined in a channel, but full understanding is still lacking. Numerous studies (both experimental [6,7] and numerical [8,9]) displayed a wide variety of behaviors, sometimes incompatible with one another [10]. When a granular material is poured on a bumpy inclined surface confined between sidewalls, two limiting flow regimes are observed. At low flow rates, the material is mobilized all the way to the base [6,8]. Above a minimum flow rate, a heap resembling a wedge forms at an inclination exceeding the angle of repose of a static pile. This "Super-Stable Heap" (SSH) is made possible by a relatively thin rectilinear layer of constant thickness riding on its surface and confined between the two frictional walls (Fig. 1(a)). It was shown in the literature [11] that a SSH is dynamically stabilized by the flow at its surface and that solely sidewall friction is responsible for its formation. Using a balance of momentum for a mobilized layer, one can derive [11] an approximate linear scaling law linking the free surface angle, φ, the height of the layer, h, and the width of the channel, W:

$$\tan\varphi = \mu_i + \mu_w \frac{h}{W}, \tag{1}$$

where μ_i and μ_w are effective friction coefficients [11]. Thus, confining walls play a major role in the momentum balance if the second term on the right in this equation dominates over the first.

* Corresponding author.
E-mail address: nicolas.taberlet@univ-rennes1.fr (N. Taberlet).

0898-1221/$ - see front matter
doi:10.1016/j.camwa.2007.04.013

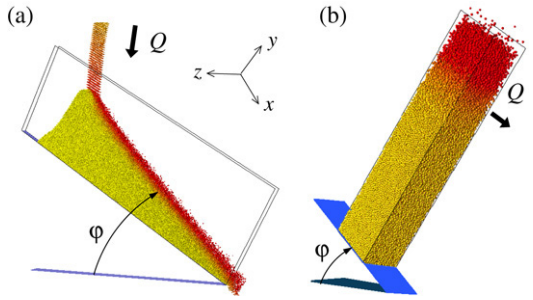

Fig. 1. Velocity based grayscale: black = fastest grains, white = slowest grains. (a) Full System (FS): grains are dropped at a constant flow rate Q into a channel confined between walls. At the exit, grains experience free fall. (b) Periodic Boundary Conditions (PBC): grains are placed in a box with the same bottom and sidewalls as the FS. Initially, grains have no velocity. The cell is then inclined at the angle φ, which triggers a flow that evolves freely toward a steady state. Fully developed flow occurs over a wide range of angles, $38^\circ < \varphi < 65^\circ$, for parameters given in the text.

2. Numerical methods

We study the phenomenon with numerical simulations based on molecular dynamics [12]. The method is described in a previous paper [13] and we briefly recall its main characteristics here. It deals with soft spheres and includes friction and rotation. Let us consider two overlapping spheres i and j. The overlap δ leads to a normal force $F_n = k_n\delta + \gamma_n\dot{\delta}$, where k_n is a spring constant, γ_n a viscous damping. The damping is used to obtain an inelastic collision. The tangential force used is that of the well-known regularized Coulomb law $F_t = \min(\mu F_n, \gamma_t v_t)$ where μ is friction coefficient, γ_t a viscous regularization constant and v_t the sliding velocity of the contact. The following values of the parameters are used: particle diameter $d = 8$ mm, mass $= 0.16$ g, $k_n = 40\,000$ N m^{-1}, $\gamma_n = 1$ kg s^{-1}, $\gamma_t = 5$ kg s^{-1} and $\mu = 0.8$. These values lead to a restitution coefficient $e = 0.4$. This value is rather small but the flow properties were found, for the most part, to be independent of e. Different values of the latter were tried but affected only the gaseous ballistic layer close to the free surface. This is consistent with earlier observations that, in dense grain assemblies, the effective restitution coefficient nearly vanishes, regardless of material properties [14]. Impacts against the sidewalls are treated as collisions with a sphere of infinite mass and radius, which mimics a large flat surface. The bottom is made bumpy with cylinders perpendicular to the flow. The granular material is made slightly polydisperse (the distribution of the grain diameter is uniform between $0.8d$ and $1.2d$) to avoid crystallization. Our simulations contain a very large number of particles, between 10^5 and 10^6, and typically run for 10^7 time steps.

Although the SSH in Fig. 1(a) forms on a rigid bumpy surface that is not inclined as steeply as the flowing layer, we find that it is possible to carry out analogous simulations with periodic boundaries perpendicular to the flow direction (Fig. 1(b)). This establishes the rectilinear SFD character of the flowing layer, and suggests substantial economies in the number of spheres necessary to run meaningful simulations.

In the full system of Fig. 1(a), as we impose a constant number flow rate Q above a critical value [11], grains get trapped underneath the flowing layer, and the SSH grows slowly [13] until its free surface reaches a steady angle φ. With periodic boundary conditions (Fig. 1(b)), we set the inclination instead, and Q evolves toward the same steady state as that of the whole SSH. Surprisingly, in the periodic system, grains below the flowing layer remain nearly immobile despite the steep inclination. Thus, the confining walls permit the establishment of a stable equilibrium on the erodible heap at an angle far exceeding what is observed without them. Nonetheless, above an angle $\varphi_{\max}$, grains accelerate, and, below $\varphi_{\min}$, they come to rest. These critical inclinations of the flowing layer are functions of simulation parameters. Remarkably, they also depend on the relative channel width (W/d), even though the grain diameter d does not appear explicitly in Eq. (1). Under present conditions $\varphi_{\min} = 38^\circ$ and $\varphi_{\max} = 65^\circ$ with $W = 5d$. In both systems, Q is measured by counting the number of grains flowing through a surface perpendicular to the confining walls per unit time. Note that, in periodic simulations, we observed that flow properties became insensitive to the domain length L along the streamwise direction when $L > 10d$. Therefore, all the periodic simulations were run using $L = 25d$.

As Fig. 2 shows, the full system and its periodic counterpart have equivalent overall flow characteristics. The flow rate vanishes for $\varphi < \varphi_{\min}$. At steeper inclinations, Q becomes a linear function of $\tan\varphi$. This behavior resembles a jamming transition [15,16], near which the system can exhibit both hysteretic and intermittent behaviors [17]. Thus, μ_{jam} may be related to the angle of repose, the angle of avalanche (maximum angle of stability), h_{stop} [6] or h_{freeze} [18].

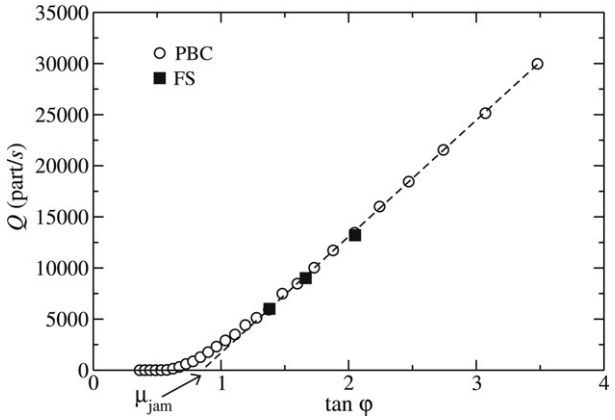

Fig. 2. Flow rate Q versus tangent of the angle of inclination of the free surface for $W = 5d$. Beside falling on the same curve, the FS and PBC simulations exhibit the same depth profiles of velocity and solid packing fraction. Therefore, the two techniques are equivalent. Here, the jamming transition occurs at $\mu_{\text{jam}} = \tan 38°$.

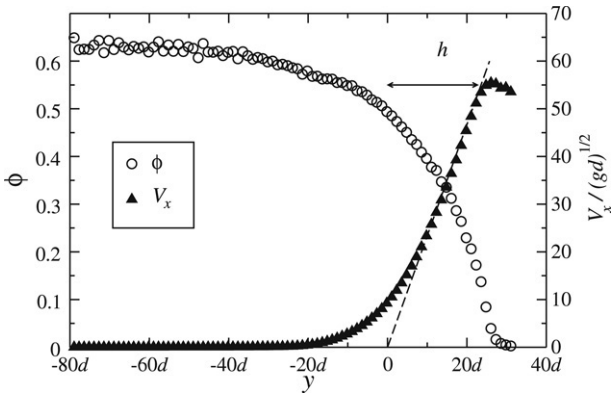

Fig. 3. Velocity and solid packing fraction profiles for $\varphi = 45°$ and $W = 20d$. The velocity profile exhibits three regions: it levels off in a tenuous region above the free surface ($y > 23d$), stays mostly linear in the flowing layer ($0 < y < 23d$), and decays exponentially within the SSH ($y < 0$). A fit to the linear part of the flowing layer defines the height h of the flow. The packing fraction decreases smoothly throughout the whole flowing layer and is nearly constant within the SSH where it corresponds approximately to the random close packing. Note that Φ can be fitted by an exponential law (see Louge et al. in this volume).

The equivalence of the full system and its periodic counterpart demonstrates that the flowing layer is SFD. Without periodic boundaries, which mimic an infinitely long flow, it is always unclear whether a physical experiment or its complete simulation have reached such a condition. Here instead, we find that all parameters of the periodic system, including its overall kinetic energy, reach a steady state. To our knowledge, this work is the first numerical simulation of steady flows over an erodible base using periodic boundary conditions. This last statement raises a question: is the presence of frictional sidewalls necessary for obtaining steady and fully developed flows over erodible piles?

3. Flow regimes

Fig. 3 shows profiles of streamwise velocity V_x and solid packing fraction ϕ averaged over time and channel width. While the velocity, made dimensionless with the gravitational acceleration g and the grain diameter, is similar to that observed experimentally [11], an important new result is that the packing fraction decreases steadily throughout the flowing layer until it nearly vanishes in the agitated surface layer. This behavior is fundamentally different from that of granular flows mobilized on a rigid, bumpy base without confining walls, which are SFD at much lower angles than the SSH, and for which Φ is invariant through most of the depth, but vanishes abruptly near the free surface [8,9].

Because the simulations of Silbert [8] and Prochnow [9] only differ from our periodic system by their absence of confining walls, the new regime described here must derive from the latter. Moreover, because our simulations with

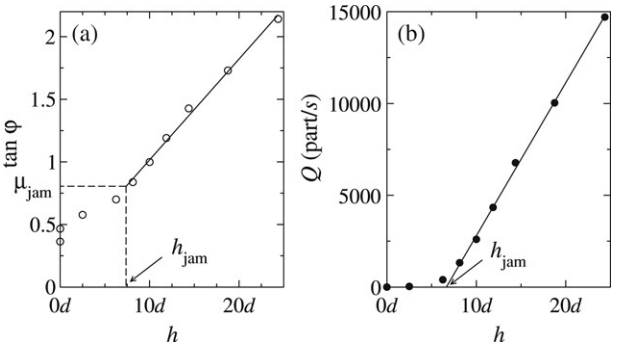

Fig. 4. (a) $\tan\varphi$ versus h for $W = 5d$. The critical value μ_{jam} found in Fig. 2 corresponds to $h = h_{\text{jam}}$. The solid line is a linear fit to the curve with $\mu_w = 0.40$ and $\mu_i = 0.21$. (b) Q versus h. Above the critical value h_{jam}, Q is a linear function of h. The solid line is a linear fit to this part of the curve.

frictionless walls produce flows at low angles $15° < \varphi < 25°$ that are identical to those of Silbert [8], except in a narrow region near the walls where geometrical exclusion plays a role, we conclude that the walls affect the flow mainly through friction, rather than through the confinement that they impose. In short, it is friction on the confining walls that stabilizes a heap at high inclinations, and that produces the peculiar profiles reported in Fig. 3.

Ancey [10] observed similar packing fraction profiles in experiments on confined flows over a rigid bumpy base, but did not recognize their origin in sidewall friction. By involving a small enough number of grains to mobilize the full or periodic systems all the way to the base, we can reproduce Ancey's observations in our simulations as well. Like their counterparts on the erodible heap, these flows depend crucially on wall friction and, as in Fig. 3, display packing fractions that increase with distance from the free surface. Such variations are therefore not intrinsic to an erodible base. Therefore, any model aiming to describe a flow with confining walls should explicitly take their presence into account.

4. Flow regime criterion

The major adjustments in packing fraction that wall friction provokes are accompanied by equally significant changes in the relation between Q and h. For flows mobilized on a bumpy surface unaffected by sidewalls, there is a range $h > h_{\text{stop}}$ in which SFD flows exist and where the flow rate satisfies $Q \propto h^{5/2}$, which was confirmed experimentally [6] in the case of wide systems. Here instead, Fig. 4 shows that, in agreement with Eq. (1), $\tan\varphi$ is a linear function of h/W above the jamming transition $h > h_{\text{jam}}$, and that Q is a linear function of height, $Q \propto (h - h_{\text{jam}})$. It should be pointed out that this curve is obtained for a very thin channel ($W/d = 5$) for which strong geometrical effects are expected.

Equation (1) can be used to delineate the two kinds of flows. To that end, we introduce the parameter $\xi = (\mu_w h)/(\mu_i W)$. When $\xi \ll 1$, confining walls are unimportant, and the flow behaves as described by Pouliquen [6], Silbert [8], and Louge [5]. On the other hand, when $\xi \geq 1$, the flow has the character shown in Figs. 1–4. Such behavior can be achieved by increasing friction on the confining walls, by raising the flow height, or narrowing the channel.

5. Conclusion

In this article, we have attributed the peculiar stabilization of a steep pile by a flowing surface layer to the friction exerted by the confining walls on the flow. Our periodic simulations over an erodible bed have established that the flow in the layer is fully developed and steady. In this regime, we have shown that the depth profiles of velocity and solid packing fraction, as well as the relation between flow rate and flow height, differ fundamentally from those for flows on a rigid bumpy base without confining walls. One can easily conceive that frictional sidewalls are responsible for an increase in the stability of granular piles [18,19] and flows [11]. Yet, the fundamental and non-trivial changes that they induce in the properties of the flow and in the rheology remain a puzzle. Theoretical attempts to understand and describe this phenomenon should explicitly include the friction on the sidewalls.

References

[1] H. Jaeger, S. Nagel, R. Behringer, Review of Modern Physics 68 (1996) 1259.
[2] T. Drake, Journal of Fluid Mechanics 225 (1991) 121.
[3] J. Rajchenbach, Physical Review Letters 90 (2003) 144302.
[4] P. Johnson, P. Nott, R. Jackson, Journal of Fluid Mechanics 210 (1990) 501.
[5] M. Louge, Physical Review E 67 (2003) 061303.
[6] O. Pouliquen, Physics of Fluids 11 (1996) 542.
[7] E. Azanza, F. Chevoir, P. Moucheront, Journal of Fluid Mechanics 400 (1999) 199.
[8] L. Silbert, D. Ertas, G.S. Grest, T. Halsey, D. Levine, S.J. Plimpton, Physical Review E 64 (2001) 051302.
[9] M. Prochnow, Ph.D. Thesis, ENPC, Marne la Vallée, 2002.
[10] C. Ancey, Physical Review E 65 (2002) 011304.
[11] N. Taberlet, P. Richard, A. Valance, W. Losert, J.-M. Pasini, J.T. Jenkins, R. Delannay, Physical Review Letters 91 (2003) 264301.
[12] J. Schaefer, S. Dippel, D. Wolf, Journal de Physique I 6 (1996) 5.
[13] N. Taberlet, P. Richard, E. Henry, R. Delannay, Europhysics Letters 68 (2004) 515.
[14] E. Falcon, C. Laroche, S. Fauve, C. Coste, The European Physical Journal B 5 (1998) 111.
[15] A. Liu, S. Nagel, Nature 396 (1998) 21.
[16] C. O'Hern, L. Silbert, J. Liu, S. Nagel, Physical Review E 68 (2003) 011306.
[17] P.-A. Lemieux, D.J. Durian, Physical Review Letters 85 (2000) 4273.
[18] S. Courrech du Pont, P. Gondret, B. Perrin, M. Rabaud, Europhysics Letters 61 (2003) 492.
[19] C. Liu, H. Jaeger, S. Nagel, Physical Review A 43 (1991) 7091.